Supplementary – Optical Particle Counter Calibration

This appendix summarizes laboratory investigations of the response of two optical particle counters to calibration particles; specifically laboratory measurements of particle size and concentration conducted in 2008 and 2011. The instruments investigated are the FSSP300 and the PCASP; both for attachment external to an aircraft fuselage and both owned by the National Center for Atmospheric Research (NCAR). During two intervals, in 2008 and 2011, these OPCs were installed on the NSF-NCAR C130 aircraft for the VOCALS (October and November, 2008) and ICET (June and July, 2011) campaigns. The FSSP300 and PCASP were fabricated by Particle Measurement Systems (PMS Inc.), a predecessor of Droplet Measurement Technologies (DMT, Inc.) which currently services both instruments.

An example of a FSSP300 measurement of laboratory-generated aerosol is shown in Figures 1a-1b. These results were provided by DMT. As we will see, there is a noticeable difference between these DMT measurements, in particular the distribution width, and what we are able to achieve in our laboratory with a different aerosol preparation methodology. Figure 1a shows the size distribution presented as a histogram of particle count, and Figure 1b presents the distribution formulated as the ratio of the channel count divided by the logarithmic difference of the particle diameter at the channel boundaries. The latter presentation is commonly used in the atmospheric and aerosol sciences (Rogers and Yau, 1989; Seinfeld and Pandis, 1998). Channel number is indicated in both figures and the nominal size of the test particles (740 nm polystyrene latex) is indicated by a vertical dashed line in Figure 1b.

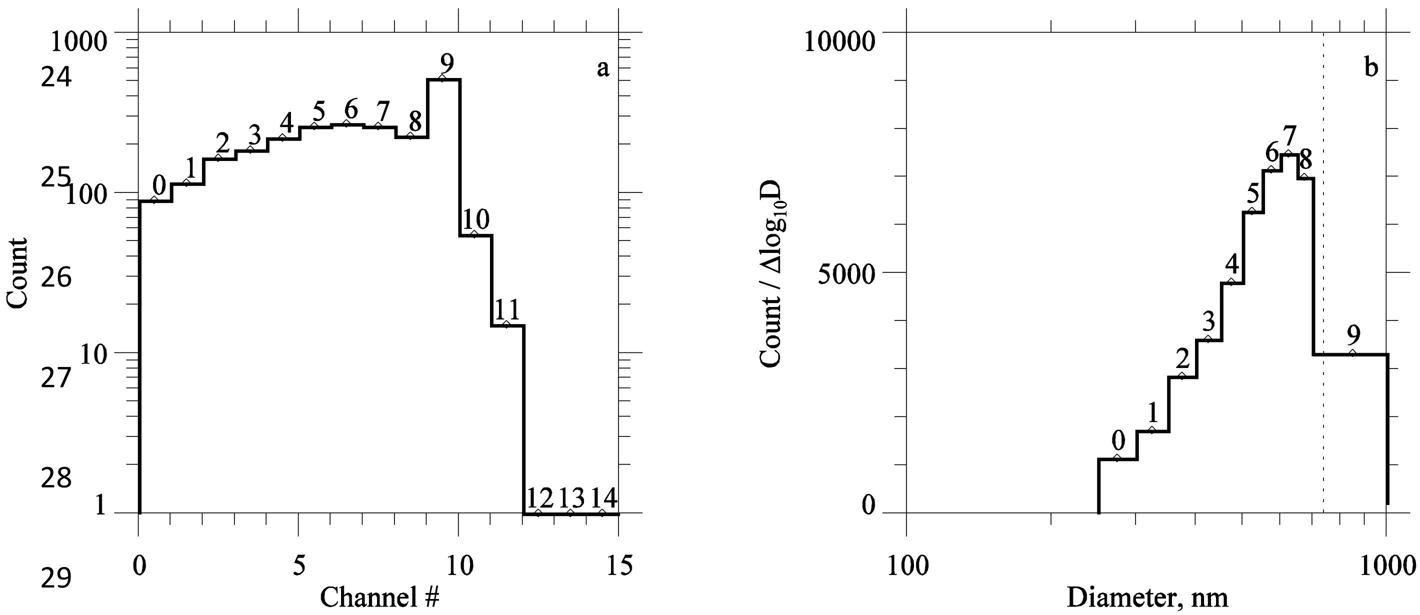

Figure 1 – FSSP300 measurements of a test particle size distribution recorded at DMT on 20070706. a) Histogram representation, b) histogram values divided by the logarithmic difference of the particle diameters at the channel boundaries. In (b) the nominal particle diameter (740 nm PSL, dashed vertical line) is also indicated. Channel numbers are illustrated in both panels.

S1 - Overview

Measurements were made in the Department of Atmospheric Science at the University of Wyoming. The aerosol generation system and the aerosol detection instrumentation are shown in Figure 2. All of the optical particle counter (OPC) testing was conducted using particles which were size-selected based on their electrical mobility. Test aerosol preparation started with pneumatic atomization of a hydrosol containing polystyrene latex (PSL) spheres. The resulting dispersion was dried, charge neutralized, size classified in a differential mobility analyzer (DMA) and diluted. In addition to a size distribution measurement made by the OPCs (FSSP300 and PCASP), the distribution was measured with a scanning mobility system and its size-integrated concentration was measured with a condensation particle counter (CPC).

S2 - Data Acquisition

The count histograms produced by the FSSP300 were recorded via the Particle Analysis and Collection Software (PACS, DMT Inc.); a histogram was recorded every second (1 Hz sampling). A size distribution was also obtained using the Scanning Mobility Particle Sizer (Scanning SMPS in Figure 2). That distribution was acquired via the Aerosol Instrument Manager (TSI Inc.) software and was recorded as a 300 s average. In addition, a Labview Virtual Instrument (National Instruments, Inc.) acquired measurements of size-integrated concentration (CPC), aerosol flowrate (TSI 4010) and the PCASP size distribution. Those three signals were sampled at 1 Hz. The three data files - PACS, AIM and Labview – were analyzed using the Interactive Data Language (ITT, Inc.).

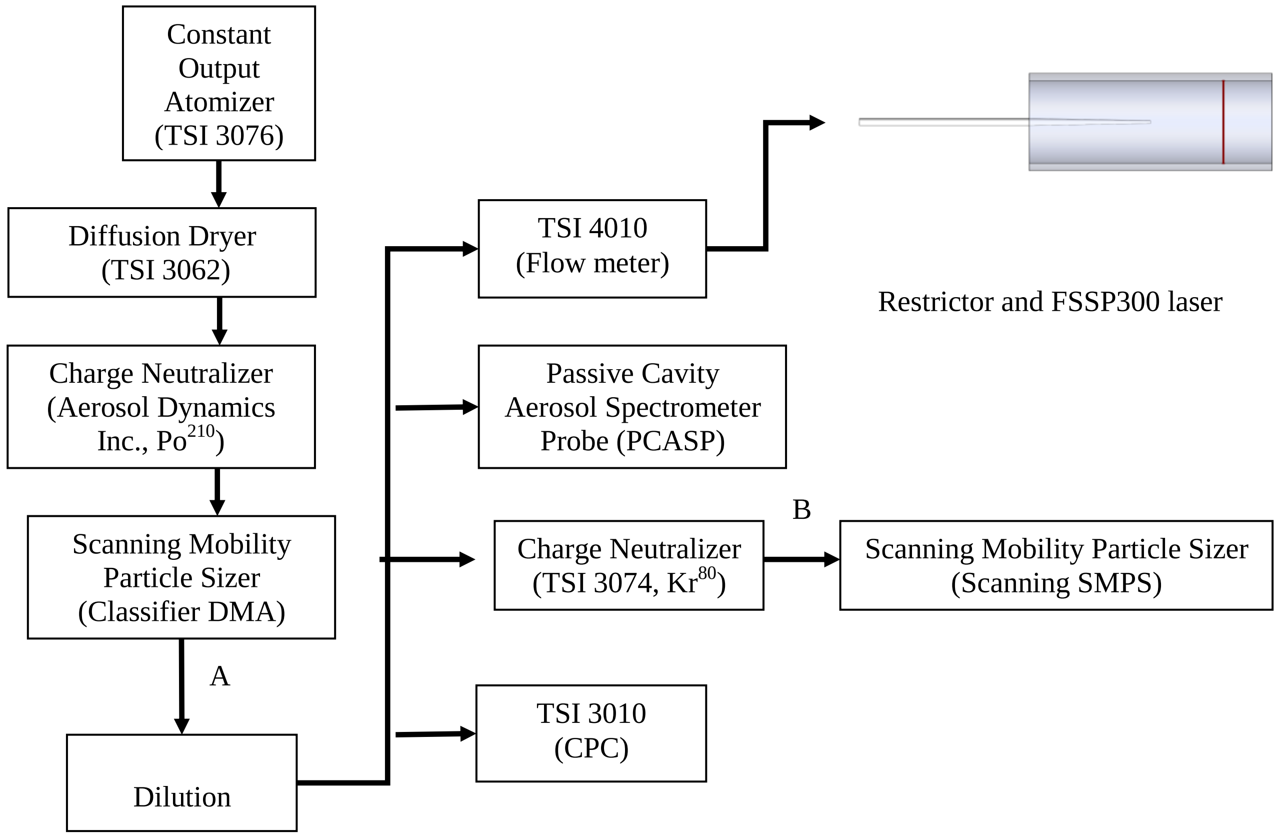

Figure 2 – Schematic of particle generation and measurement systems.

S3.1 - FSSP300

Figure 2 shows that a convergent tube - 3 mm to 1 mm inner diameter - was used to accelerate the aerosol flow through the FSSP300's laser. We refer to the tube as the restrictor and note that a flow meter was used to monitor the flowrate through the restrictor. Testing revealed no significant particle loss in either the restrictor or the flow meter (343 to 707 nm diameter PSL particles). Particle velocities at the outlet of the restrictor were varied between 2 and 25 m/s by controlling the air stream's flowrate.

S3.2 - FSSP300 Sample Area

An outstanding problem with the FSSP300 is the difficulty of measuring the portion of the laser beam known as its sensitive volume. Particles crossing through the sensitive volume produce an in-focus scattering pattern at the FSSP300's photodetector, and those that do not produce an out-of-focus pattern. These two possibilities (in-focus and out-of-focus) are distinguished by the probe's microprocessor, in real time, by comparing of signals reported by a partially masked, and an unmasked photodetector (Baumgardner et al., 1992).

During airborne operation, one dimension of the sensitive volume is known from determinations of the C130's true air speed and the probe's sampling rate. The other two dimensions are an optical depth-of-field, measured along the axis of the laser, and a transverse dimension, commonly known as the laser beam height. The product of the depth-of-field and the beam height define the probe's sensitive area. Baumgardner et al. (1992) evaluated the sensitive area by correlating the particle count, reported by the FSSP300, with particle concentration values reported by a FSSP100. More recently, we determined the sensitive area by correlating measurements of the FSSP300 count and PCASP concentration (Snider and Petters, 2008). Because the restrictor we employed has a 0.8 mm^2 crossection, significantly larger than the FSSP300's sensitive area, the laboratory measurements reported here cannot be used to estimate the sensitive area. For the VOCALS campaign (October and November 2008) we applied the technique of Snider and Petters (2008) and determined a value 0.15 mm^2 for the FSSP300's sensitive area.

S3.3 - FSSP300 Laboratory Test Data

FSSP300 measurements of test particle size distributions are provided in Figure 3 (http://www.atmos.uwyo.edu/~jsnider/spring_2012/smps_nc_processor_cpc_f300_smps_10.pdf)

This figure is a composite of 59 tests, all conducted in our laboratory. Results are arranged chronologically from May 2009 to August 2011; tests with particle diameters equal to 343, 491 and 707 nm are reported. Included, for each test, are size distributions (300 s average), from the scanning SMPS and FSSP300 (left panel), and the count histogram from the FSSP300 (right panel, also a 300 s average). The vertical dashed line (left panel) is the diameter of the PSL particles. The latter is set by the PSL size we place in the atomizer (Figure 2), and by the manufacturer's specification (Duke Scientific Inc.) of the particle's monodisperse size. The latter is the particle diameter we set in the classifier DMA (Figure 2).

We obtained good agreement between the PSL diameter (D_{PSL}) and the mode diameter reported by the scanning SMPS (D_{SMPS}). When expressed as an absolute relative standard deviation this agreement evaluates as

$$\left(\frac{\sum(x_i-\bar{x})^2}{N}\right)^{0.5}=0.01 \qquad \text{where } x_i=\frac{\left|D_{PSL,i}-D_{SMPS,i}\right|}{D_{PSL,i}} \text{ and } N=59 \qquad (1)$$

The latter demonstrates that the average departure between Duke Scientific's estimate, and our SMPS-based estimate of the particle size, is 1 part in 100. From Figure 3 it is possible to make comparisons between the PSL diameter (D_{PSL}) and the mode diameter reported by the FSSP300 (D_{FSSP}). When formulated as Equ. 1, that departure is 6 parts in 100

$$\left(\frac{\sum(x_i - \bar{x})^2}{N}\right)^{0.5} = 0.06 \qquad \text{where } x_i = \frac{\left|D_{PSL,i} - D_{FSSP,i}\right|}{D_{PSL,i}} \text{ and } \quad N=59 \qquad (2)$$

From Figure 3 two additional conclusions are possible. The first is related to particle charge state within the aerosol generation system. At point "A" (Figure 2) most of the test particles are singly-charged and most have a diameter equal to the prescribed PSL diameter. While on their way to the scanning SMPS, the particles pass through a neutralizer, where a Boltzmann charge state is reestablished (TSI, 2003). Subsequent to the neutralizer, and prior to entering the cylinder of the scanning SMPS, at point "B", the +1 particles are present with multiply-charged particles (+2, +3, etc.). From knowledge of the particle's diameter, the mean free path of air and the Cunningham slip correction factor (Snider et al., 2010), we calculated the mobility-equivalent diameter of the multiply-charged particles. Those diameters are indicated with arrows in the left-panels of Figure 3. Examination of Figure 3, particularly the last 10 distributions of Figure 3, demonstrates that the particles detected by the scanning SMPS, at sizes smaller than D_{PSL}, actually have a diameter equal to D_{PSL}. Such ambiguity is a consequence of the SMPS's discrimination of particles based on their electrical mobility, and the fact that electrical mobility depends on both particle's diameter and its charge state.

Our second finding relates to a user-selectable option for FSSP300 measurements acquired by the Particle Analysis and Collection Software (PACS). When setting up PACS the user can select either "yes" or "no" for the option Reject-Based-on-Depth-of-Field. If "yes" is selected, then a subset of particle detections is recorded by PACS, and if "no" is selected, all detections are recorded. An example size distribution, acquired with the option set to "no", is shown in the first test of Figure 3, where it is evident that most of the detections were classified in channel 0. By comparing this to a test with "yes" selected, and with the same D_{PSL} (491 nm), we infer that the in-focus detections (first test of Figure 3) correspond to the minor FSSP300 mode at channel 5. In our data set of 57 experiments we have 37 and 22 experiments with the Reject-Based-on-Depth-of-Field option set to "yes" (in-focus detections only) and "no" (both in-focus and out-of-focus detections), respectively.

S3.4 - FSSP300 Counting Efficiency

Concentrations obtained from the CPC were used to derive the counting efficiency of the FSSP300. The efficiencies were derived as the ratio of the FSSP300 count divided by the product of the CPC concentration and flowrate (Figure 2). The latter was derived from the measurement mass flowrate multiplied by the ratio of sea-level pressure (1013 hPa) and the pressure in Laramie (780 hPa). The derived efficiencies are averages of 300 samples (1 Hz acquisition) and the averaging interval is the same as the averaging interval for size distributions from the scanning SMPS (Figure 3). Averaged efficiencies are 0.08±0.02 (yes=Reject-Based-on-Depth-of-Field, # = 37) and 0.71±0.47 (no=Reject-Based-on-Depth-of-Field, # = 22). The first average indicates that only a subset of detections (~8%) corresponds to in-focus detections. This finding is consistent, at least qualitatively, with the fact that the FSSP300's sensitive area (0.15 mm^2) is small relative to the restrictor's 0.8 mm^2 crossection. Quantitative agreement between these two results would require an accounting of the spreading of the aerosol beam between the restrictor and the laser. Efficiencies corresponding to 343 and 491 nm particles and the "yes" option, were similar (0.09±0.01 (#=7) and 0.08±0.02 (#=22), respectively; however, smaller efficiencies were documented for 707 nm particles (0.04±0.01 (# = 8)). Smaller counting efficiencies for the 707 nm particles is not understood.

S3.5 - FSSP300 Size Calibration

Size distributions corresponding to the “no” tests, and the “yes” tests, and for all test particle sizes (D_{PSL} =343, 491 and 707 nm), were analyzed. From this we conclude that the in-focus particles classify in the zeroth channel (D_{PSL} = 343 nm experiments), in channel 5 (D_{PSL} =491), and in channel 8 (D_{PSL} =707 nm).

Consistent particle sizing results were obtained for testing conducted in 2008 and in 2011. Figure 3 shows 14 tests with 343 nm particles, 30 tests with 491 nm particles and 15 tests with 707 nm particles. Without exception, the maximum of the histogram always occurred in the zeroth, the fifth and eighth channels, respectively.

Figure 4 summarizes the FSSP300 sizing calibrations, discussed in the previous paragraphs, and sizing calibrations performed by DMT in 2007. The instrument has two gain stages and results are split between calibrations for small particles (High Gain, Figure 4a) and large particles (Low Gain, Figure 4b). Calibration data points are shown as triangles with gray and blue indicating calibrations conducted at WYO and DMT, respectively. The threshold value, shown on the abscissa, is proportional to the maximum scattering intensity of a particle classifying in a particular channel, i.e., it is an upper-limit threshold.

Assignment of an array of thresholds to an array of diameters is possible theoretically, via Mie scattering theory, provided the basic properties of the instrument (scattering geometry and signal amplification) is known. That assignment is often referred to as the factory calibration.

The latter is shown in Figure 4 by a dashed line connecting small diamonds plotted at each of the 30 diameter-threshold pairs. Overall, we document good agreement between the WYO and DMT data points and the factory calibration. Given that agreement we see no reason to revise the size-threshold relationship for the FSSP300.

The work summarized in the previous paragraph is based on measurements made in our laboratory with the FSSP300 initialized with the factory size-threshold table. When the instrument is operated on the NCAR C-130 a non-conventional size-threshold table is used (private communication David Rogers, April 16, 2009). The C-130 threshold-size table is presented below Figures 4a and 4b, and the red-dashed lines, in the figures, indicate the interpolation used to derive the calibration diameter as a function of threshold. The derived diameters are archived in the Network Common Data Format (NetCDF) files released by NCAR for ICET (June and July, 2011). For the VOCALS campaign (October and November, 2008), the diameters in the NetCDF file are 4 to 50% larger than the recommendation provided in Figure 4. Users of both the VOCALS and ICET data sets are encouraged to use the threshold-size table presented below Figures 4a and 4b.

S3.6 - FSSP300 Size Distribution Width

We now compare the width of the size distribution corresponding to the DMT and the WYO particle generation methodologies. The former uses the same supplier for the test particles (Duke Scientific Inc.) but does not size-select the test particles in a classifier DMA. Looking back at Figure 1b (DMT methodology), the width of distribution, at half height, is 5 channels (#4, #5, #6, #7 and #8). For the UWYO methodology, and approximately the same particle diameter, the width is substantially smaller, at most one channel. Two examples of this can be seen in Figure 3 by starting at the last test and counting backwards twelve and thirteen distributions.

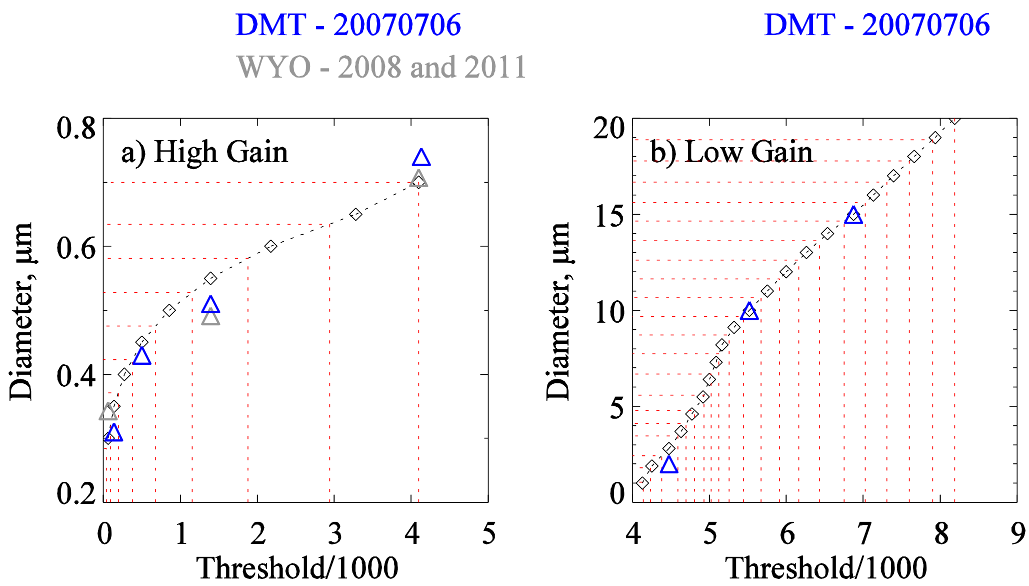

38	0.284
92	0.320
194	0.371
376	0.423
678	0.475
1155	0.528
1880	0.581
2942	0.635
4096	0.700

4140	1.060
4238	1.795
4384	2.430
4590	3.449
4699	4.112
4807	4.792
4928	5.578
5027	6.668
5124	7.728
5255	8.717
5446	9.665
5673	10.651
5912	11.636
6164	12.623
6429	13.614
6754	14.647
7027	15.595
7310	16.683
7601	17.776
7901	18.876
8192	20.000

Figure 4 – Summary of laboratory determinations of FSSP300 sizing performed at DMT and at the University of Wyoming (WYO). The recommended size-threshold table for the NCAR C-130, assuming refractive index 1.59 spheres, is also provided. See text for details.

S4.1 - PCASP

Figure 2 shows the PCASP with the scanning SMPS and the CPC. Sections S3.1 and S3.3 discuss the PSL particle generating system.

S4.2 - PCASP Airflow and Sample Heating

The PCASP's airflow system is designed to direct an aerosol stream across the probe's Helium-Neon laser (λ=0.633 μm). Particle loss is minimized by directing the stream along a straight path from the sample inlet to the laser (Figure 5). The stream first encounters a diffuser where the flow is decelerated from the C130's true airspeed (~110 m/s) to ~11 m/s (Particle Measuring Systems, 2002). The velocity of the flow passing through the narrow tube at the back of the diffuser is determined, to first order, by the PCASP's sample flowrate and the tube's ID (0.5 mm); the velocity in this part of the inlet is ~7 m/s. Just before the flow enters the sample cavity, it is combined with the sheath air stream. The volumetric rate of the sheath stream is set to be 15 times the sample flowrate. Because of a nozzle restriction at the point where the flows are combined, the combined stream crosses the laser at approximately 45 m/s (Particle Measuring Systems, 2002). The combined stream then exits the sample cavity, passes through a pump, a tube filled with granular desiccant, a filter, and is split. One of the streams is the sheath flow, which is recirculated; the other is the sample flow. Subsequent to the sample flow needle valve, the sample stream passes through a mass flow meter (not shown), and is dumped. The device used to measure the sample flowrate is a Honeywell Mass Airflow Sensor (Model AWM3100V).

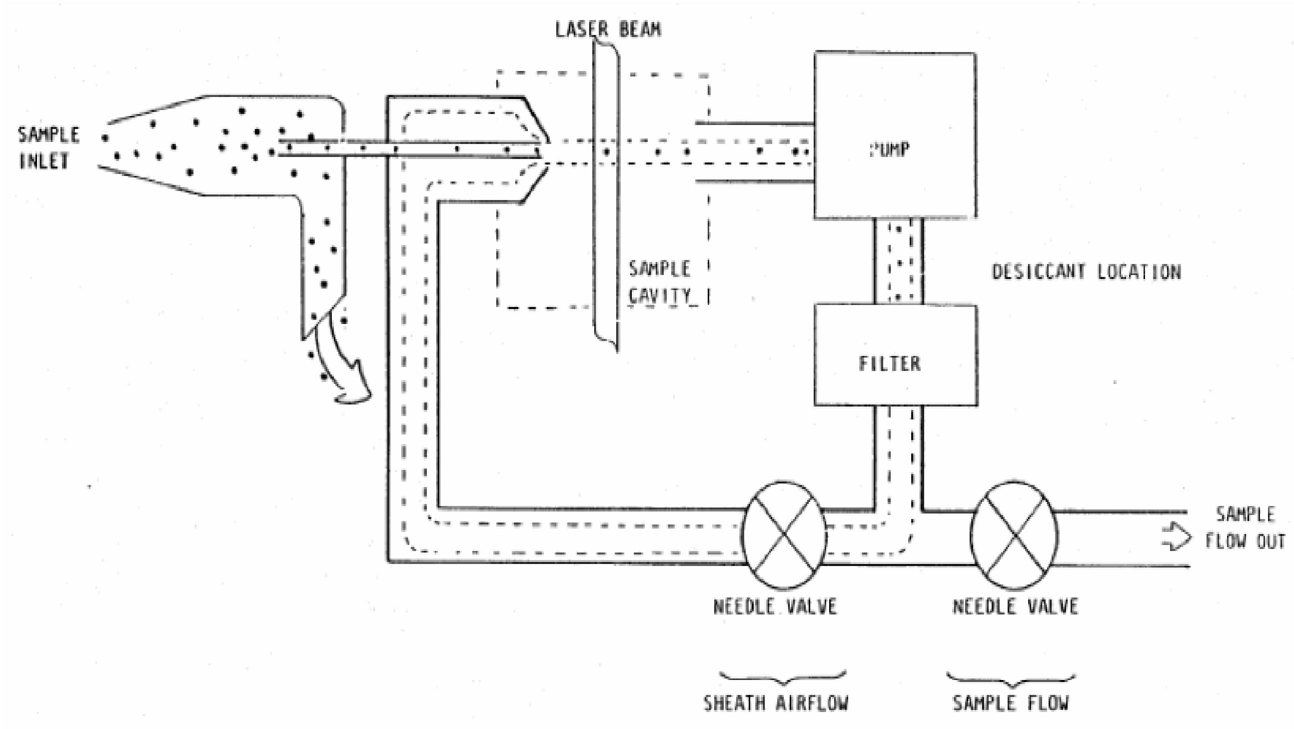

Figure 5 -The PCASP's sampling system. The sample flowmeter (not shown) is located downstream of the sample flow needle valve.

Previously we mentioned the narrow tube that carries the sample flow from the diffuser to the sample cavity. This tube is evident in Figure 5 and will be referred to as the “needle.” The PCASP inlet is equipped with three deice heaters. These are located near the tip of the diffuser (35 watt), at the base of the diffuser (100 watt), and in close proximity to the front end of the needle (10 watt). Strapp et al. (1992) demonstrated that compressional warming, with heating due to the deice heaters, can have a substantial effect on the size of wet aerosol particles. They estimate that particles reside sufficiently long within the warming stream approaching the PCASP, and within the probe, to loose most of their chemically-bound water. Strapp et al. estimate the interaction time to be 0.2 s. Snider and Petters (2008) used a model similar to that employed by Strapp et al. and showed that particles starting at a wet diameter 0.84 µm have enough time to evaporate to a diameter (0.48 µm) consistent with the relative humidity assumed for the particle trajectory (40%). The inference, coming from Snider and Petters, is that wet particles larger than ~0.8 µm are not resident long enough to evaporate to a size consistent with the particle composition and relative humidity constraints assumed in the modeling.

S4.3 – PCASP Sample Airflow Calibration

The PCASP derives particle concentration as the ratio of the particle count rate (number of particles per channel per second) and sample flowrate (actual cubic centimeter per second). The latter is derived in two steps. First, the signal from the PCASP’s sample flow sensor, represented either as an analog signal (millivolt, mV; VOCALS), or as an integer (COUNTS, ICET), is used to derive the flowrate (standard cubic centimeter per second). The project-specific calibrations are

Standard cubic centimeter per second =

$$-0.0165 + (7.9354e\text{-}05)*mV + 1.1453e\text{-}07 *mV^2 \quad \text{(VOCALS)} \quad (3)$$

and

Standard cubic centimeter per second =

$$7.51885 + (-8.46821e\text{-}3)*COUNTS + 2.30130e\text{-}6*COUNTS^2 \quad \text{(ICET)} \quad (4)$$

In the second step, the standard flowrate value is converted to the ambient flowrate, by evoking the ideal gas law and the C130's measurements of ambient pressure and temperature.

We evaluated the flowrate calibration by fitting flow measurements, from a bubble flow meter (Gilian Instrument Corporation), converted to standard pressure and temperature, and the signal output by the PCASP's flow meter (V_{out}, Volt). Signal digitization, done internally within the PCASP, is based on a twelve-bit A-to-D converter. For that device the Volt-to-COUNTS conversion formula is

$$COUNTS = V_{out} /4.88281e\text{-}3 + 2048 \quad (5)$$

The ICET flow calibration data is shown Figure 7. Lab measurements, obtained prior to and after the project, were combined to generate a calibration (Eqn. 4) for the whole ICET campaign.

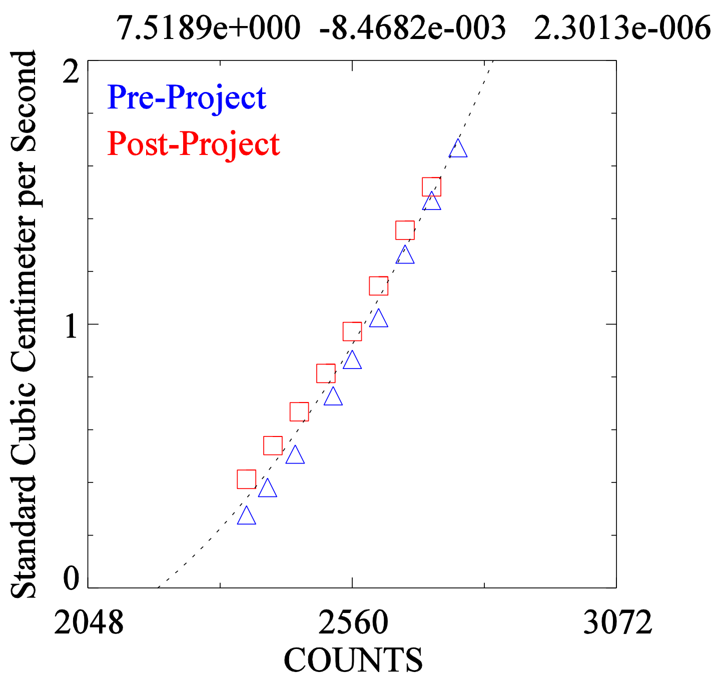

Figure 7 – ICET calibration of the PCASP sample flow meter and the second-order fit equation. Standard conditions are P_o=1013 hPa and T_o=293 K.

S4.4 - PCASP Size Calibration

PCASP size distributions were evaluated for five test particle sizes (D_{PSL} =125, 152, 199, 491 and 707 nm); results from the 47 available tests are shown in Figure 8 (http://www.atmos.uwyo.edu/~jsnider/spring_2012/pcasp_size_calibration_ncar.pdf). Here, red indicates a size distribution from the scanning SMPS and blue the distribution from the PCASP (both are 300 s averages). Also evident is a vertical dashed line, in the left panels, at the nominal size of the PSL particles and arrows indicating the mobility-equivalent diameter of the multiply-charged particles.

We obtained good agreement between the PSL diameter (D_{PSL}) and the mode diameter reported by the PCASP (D_{PCASP}). When formulated as Equ. 1, the average departure is 2 parts in 100

$$\left(\frac{\sum(x_i-\bar{x})^2}{N}\right)^{0.5}=0.02 \qquad \text{where } x_i=\frac{\left|D_{PSL,i}-D_{PCASP,i}\right|}{D_{PSL,i}} \text{ and } N=47 \qquad (6)$$

The work summarized in the previous paragraph is based on measurements made with the PCASP initialized with the factory size-threshold table. When the instrument is operated on the C-130 a non-conventional size-threshold table is used (private communication Allen Schanot, June 12, 2009). The C-130 threshold-size table is presented below Figures 4a and 4b, and the red-dashed lines, in the figures, indicate the interpolation used to derive the calibration diameter as a function of threshold. At their greatest absolute relative departure, these calibrated diameters are 87% smaller than the values released by NCAR (VOCALS), and 22% larger than the values released for ICET. More typical absolute relative departures are -12% (VOCALS) and +12% (ICET). Users of those data sets are encouraged to use the threshold-size table presented below Figures 8a-8c.

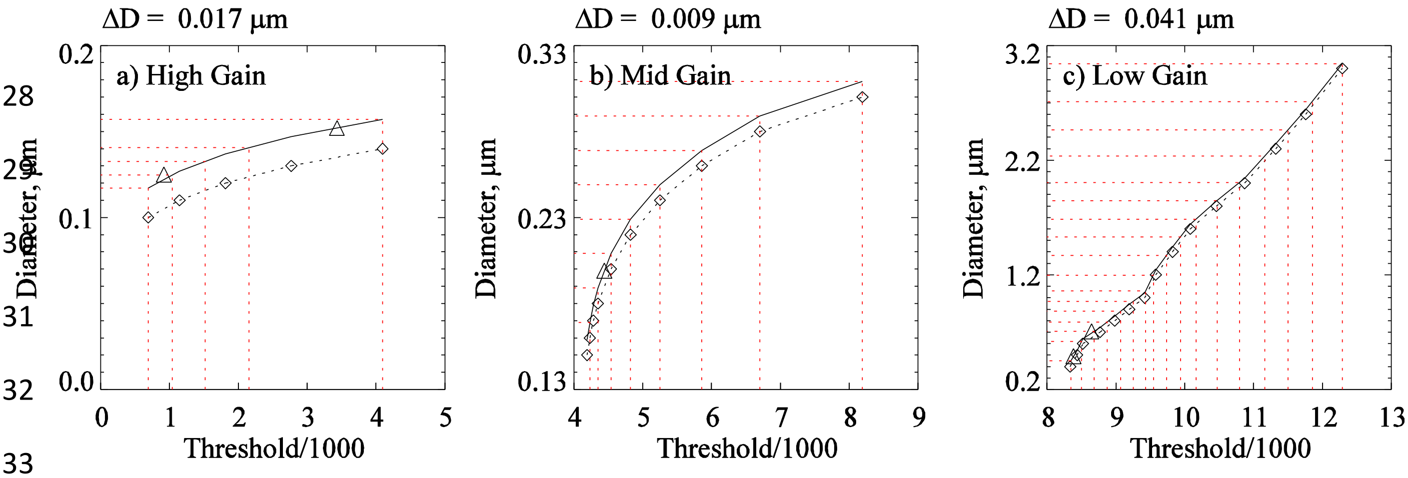

692	0.117
1040	0.125
1517	0.133
2157	0.141
4096	0.157

4231	0.169
4348	0.189
4537	0.209
4825	0.229
5251	0.249
5859	0.269
6703	0.289
8192	0.309

8345	0.451
8502	0.620
8682	0.706
8872	0.790
9070	0.883
9252	0.967
9432	1.058
9544	1.198
9737	1.369
9937	1.529
10166	1.686
10471	1.846
10797	2.005
11162	2.234
11499	2.463
11852	2.711
12288	3.041

Figure 8 – Summary of laboratory determinations of PCASP sizing performed at the University of Wyoming. The recommended size-threshold table for the NCAR C-130, assuming refractive index 1.59 spheres, is also provided. See text for details.

References

Baumgardner, D., J. E. Dye, G. B. Gandrud and R. G. Knollenberg, Interpretation of measurements made by the forward scattering spectrometer probe (FSSP-300) during the airborne arctic stratospheric expedition, J. Geophys. Res, 97(D8), 8035-8046, 1992

Particle Measuring Systems, *Passive Cavity Aerosol Spectrometer Probe (Airborne), PMS Model PCASP-100X 0.10 – 3.0 µm Operating Manual*, PMS Inc., Boulder, CO, 2002

Rogers, R.R., and M. K. Yau, *A Short Course in Cloud Physics*, 2^{nd} Edition, Pergamon Press, 1989

Seinfeld, J.H., and S.N.Pandis, *Atmospheric Chemistry and Physics*, J.Wiley, New York, 1998

Snider, J.R. and M.D.Petters, Optical particle counter measurement of marine aerosol hygroscopic growth, *Atmos. Chem. Phys.*, 8, 1949-1962, 2008

Strapp, J. W., W. R. Leaitch and P. S. K. Liu. Hydrated and dried aerosol-size-distribution measurements from Particle Measuring Systems FSSP-300 probe and deiced PCASP-100X probe, J Atmos Oceanic Technol, 9, 548-555, 1992

TSI Inc., St. Paul, Minnesota, 2000, Model 3936 SMPS (Scanning Mobility Particle Sizer) Instruction Manual